

1702. Coupling mechanism of dual-excitation fatigue loading system of wind turbine blades

Xuemei Huang¹, Lei'an Zhang², Guangming Yuan³, Na Wang⁴

College of Mechanical Engineering, Shandong University of Technology, Shandong, China

¹Corresponding author

E-mail: ¹huangxuemei@sdut.edu.cn, ²ziaver@163.com, ³yuanguangming@263.net,

⁴wangna15269309872@163.com

(Received 25 March 2015; received in revised form 10 July 2015; accepted 15 July 2015)

Abstract. A new dual-excitation fatigue loading system of wind turbine blades was designed in this paper. However, the two excitations and blade constituted a complicated non-liner energy transferring system in which the vibration coupling effect would influence the sequent accurate control of fatigue test. To study the mechanism of the coupling system mentioned above, the electromechanical coupling mathematical model was established by simplifying the loading system rationally and the factors affecting the vibration coupling were obtained accordingly. Then the simulation model of the system was built in Matlab/Simulink environment to mainly analyze the basic influence laws of the motor speed and the initial phase difference of two excitations. Finally, a small dual-excitation fatigue loading system was established to verify the correctness of the mathematical and simulation model. It could be concluded that the results of on-site test were consistent with the results of simulation.

Keywords: wind turbine blade, fatigue test, electromechanical coupling, mathematical model, numerical simulation.

1. Introduction

As an important renewable energy technology, wind power generation has many ecological and economic benefits. According to the report Technology Roadmaps – Wind energy released by International Energy Agency, by the mid-21st century, the proportion of wind power generation in global power supply will rise from the present 2 % to 12 % [1]. In a wind turbine generator, blades are the main part bearing the wind power. A large number of accidents and research results show that due to the impact of alternating load, fatigue is one of the main failure mechanisms for blades [2-3]. Thus, fatigue test of a wind turbine blade is an effective and reliable method to detect weaknesses in a blade's design [4].

Fatigue tests on blades are typically conducted by imposing an excitation mounted at 70 % of the blade length along the span wise direction and making the blade and excitation resonate together [5]. However, this test method has deficiencies of long test cycle and lacking of driving capability etc. In this paper, a dual-excitation fatigue loading system of wind turbine blades was developed to solve the problems mentioned above. However, the two excitations and blade constitute a complicated non-liner energy transferring system, in which the vibration coupling effect will influence the distribution of flexural moment and resonance of whole system and further more lead to inaccurate control of fatigue test. So the coupling mechanism of dual-excitation fatigue loading system need to be investigated.

For dual-excitation vibration system, Blekhan first proposed the synchronous control theory of dual-excitation vibration machine [6]. After that, the coupling characteristics of dual-exciter vibration mechanical system have been investigated by many researchers [7-10]. However, from the current literatures, it could be concluded that in the field of fatigue loading tests for wind turbine blades, studies on the vibration coupling mechanism of two excitors have not been carried out both in domestic and abroad.

2. Electromechanical coupling mathematical model of the dual-excitation fatigue loading system of wind turbine blades

2.1. Establishing the mathematical model the mechanical vibration system

The dual-excitation fatigue loading test system consisted of a loading test base, wind turbine blade and fatigue loading equipment. The root of the blade was fixed by high strength screw bolts to the loading base which was mounted on the ground. Two set of fatigue loading equipment were mounted on the blade along the span wise direction. The fatigue loading equipment mainly included an unbalanced shaft, three-phase asynchronous motor, fixture, gear box, and electric control equipment. The fatigue loading system is shown in Fig. 1.

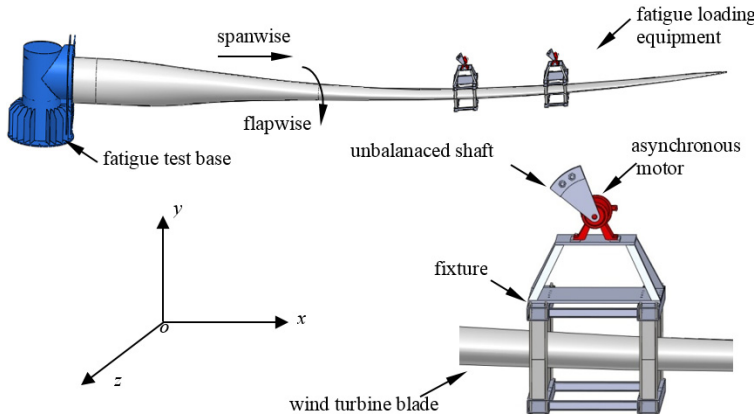


Fig. 1. Dual-excitation fatigue loading system of wind turbine blades

The dynamic model of the dual-excitation fatigue loading system is shown in Fig. 2. In order to simplify the system, it was assumed that the damping force suffered by the blade in each direction was a linear function of the velocity, and the elastic force was also a linear function of the displacement.

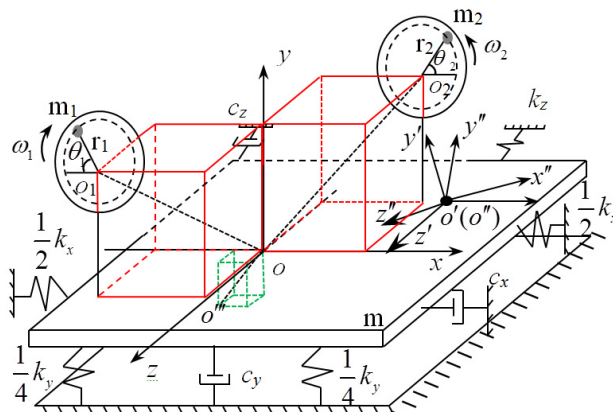


Fig. 2. Dynamic model of dual-excitation fatigue loading system of wind turbine blades

In Fig. 2, $oxyz$ is the absolute coordinate system, $o'x'y'z'$ and $o''x''y''z''$ are the moving coordinate system, o''' is the centroid of the whole vibration system (include the blade and the two set of loading equipment), m is the total weight of the blade and two sets offatigue loading equipment. o_i is the rotary center of the unbalanced shaft i , m_i is the weight of the unbalanced

shaft i , r_i is the equivalent arm length of the unbalanced shaft i , θ_i and ω_i are the rotary angle and angular velocity of the the unbalanced shaft i and $\omega_i = \dot{\theta}_i$ ($i = 1, 2$).

x, y, z, φ_i and θ_i ($i = 1, 2$)were regarded as generalized coordinates, then according to Lagrange equation[11], the dynamic equation of the dual-excitation fatigue loading system is established as follows:

$$\left\{ \begin{array}{l} \left(m + \sum_{i=1}^2 m_i \right) \ddot{x} + k_x x + c_x \dot{x} = 0, \\ \left(m + \sum_{i=1}^2 m_i \right) \ddot{y} + \sum_{i=1}^2 m_i r_i (\ddot{\theta}_i \cos \theta_i - \dot{\theta}_i^2 \sin \theta_i) + k_y y + c_y \dot{y} = 0, \\ \left(m + \sum_{i=1}^2 m_i \right) \ddot{z} + k_z z + c_z \dot{z} = 0, \\ \left(ml_{01}^2 + \sum_{i=1}^2 m_i l_{i1}^2 + J_{01} \right) \ddot{\varphi}_1 + (ml_{01} l_{02} \sin \beta_{01} \sin \beta_{02} \right. \\ \quad \left. - \sum_{i=1}^2 m_i l_{i1} l_{i2} \cos \beta_{i1} \cos \beta_{i2}) \ddot{\varphi}_2 + k_{\varphi_1} \varphi_1 + c_{\varphi_1} \dot{\varphi}_1 \\ = \sum_{i=1}^2 m_i r_i l_{i1} \cos \beta_{i1} (\ddot{\theta}_i \cos \theta_i - \dot{\theta}_i^2 \sin \theta_i), \\ \left(ml_{02}^2 + \sum_{i=1}^2 m_i l_{i2}^2 + J_{02} \right) \ddot{\varphi}_2 + (ml_{01} l_{02} \sin \beta_{01} \sin \beta_{02} \right. \\ \quad \left. - \sum_{i=1}^2 m_i l_{i1} l_{i2} \cos \beta_{i1} \cos \beta_{i2}) \ddot{\varphi}_1 + k_{\varphi_2} \varphi_2 + c_{\varphi_2} \dot{\varphi}_2 \\ = \sum_{i=1}^2 m_i r_i l_{i2} \cos \beta_{i2} (\ddot{\theta}_i \cos \theta_i - \dot{\theta}_i^2 \sin \theta_i), \\ J_i \ddot{\theta}_i + m_i r_i \cos \theta_i (\dot{y} + \dot{\varphi}_1 l_{i1} \cos \beta_{i1} - \dot{\varphi}_2 l_{i2} \cos \beta_{i2} + \ddot{\theta}_i r_i \cos \theta_i - \dot{\theta}_i^2 r_i \sin \theta_i) \\ = T_{m_i}, \quad (i = 1, 2), \end{array} \right. \quad (1)$$

where, φ_i is the included angle of $oxyz$ and two moving coordinate system, respectively, l_{i1} is the projection of oo_i in the plane yoz and l_{i2} is the projection of oo_i in the plane xoy . β_{i1} is the include dangle of l_{i1} and the positive direction of z -axis, β_{i2} is the included angle of l_{i2} and the positive direction of x -axis and β_{0i} is the include dangle of l_{0i} and the negative direction of y -axis, k_x, \dots, k_y, k_z and $k_{\varphi i}$ are the stiffness coefficient of x, y, z and φ_i direction, respectively, c_x, c_y, c_z and $c_{\varphi i}$ are the damping coefficient of x, y, z and φ_i direction, respectively, J_{oi} is the rotational inertia of the system around x axis and z axis, J_i is the rotational inertia of the asynchronous motor i , T_{mi} is the electromagnetic torque of the shaft of the asynchronous motor i ($i = 1, 2$ for all the parameters above). l_{01} and l_{02} are the projection of oo''' in the plane yoz and plane xoy , respectively.

2.2. The mathematical model of three-phase asynchronous motor

In the fatigue loading equipment, each unbalanced shaft was driven by a three-phase asynchronous motor, which would generate the loading force. So the mathematical model of the three-phase asynchronous-motor was also needed to be built. However, the model of asynchronous motor in the case of three-phase was complicated, so in practice, the mathematical model based on two-phase synchronous rotating coordinate system $\alpha\beta$ was applied to represent the original model in abc system [12].

The coordinate transformation equation of three-phase asynchronous motor from abc system to $\alpha\beta$ system is expressed by:

$$\begin{cases} i_\alpha = \sqrt{\frac{2}{3}} i_a - \frac{1}{2} (i_b + i_c), \\ i_\beta = \frac{\sqrt{3}}{2} (i_b - i_c). \end{cases} \quad (2)$$

The voltage equation of three-phase asynchronous motor based on $\alpha\beta$ system is expressed by:

$$\begin{cases} u_{\alpha 1} = r_1 i_{\alpha 1} + p\Psi_{\alpha 1}, \\ u_{\beta 1} = r_1 i_{\beta 1} + p\Psi_{\beta 1}, \\ u_{\alpha 2} = r_2 i_{\alpha 2} + p\Psi_{\alpha 2} + \Psi_{\beta 2}\omega_r, \\ u_{\beta 2} = r_2 i_{\beta 2} + p\Psi_{\beta 2} + \Psi_{\alpha 2}\omega_r. \end{cases} \quad (3)$$

The flux linkage equation of three-phase asynchronous motor based on $\alpha\beta$ system is expressed by:

$$\begin{cases} \Psi_{\alpha 1} = L_s i_{\alpha 1} + L_m i_{\alpha 2}, \\ \Psi_{\beta 1} = L_s i_{\beta 1} + L_m i_{\beta 2}, \\ \Psi_{\alpha 2} = L_r i_{\alpha 2} + L_m i_{\alpha 1}, \\ \Psi_{\beta 2} = L_r i_{\beta 2} + L_m i_{\beta 1}. \end{cases} \quad (4)$$

The electromagnetic torque and the load torque equation is expressed by:

$$T_e = n_p L_m (i_{\beta 1} i_{\alpha 2} - i_{\beta 2} i_{\alpha 1}), \quad (5)$$

$$T_e = T_L + \frac{J}{n_p} \cdot \frac{d\omega_r}{dt}, \quad (6)$$

where, r_1 and r_2 are the winding resistance of the stator and the rotor, $i_{\alpha 1}$ and $i_{\beta 1}$ are the terminal currents of the stator in $\alpha\beta$ system, $i_{\alpha 2}$ and $i_{\beta 2}$ are the terminal currents of the rotor in $\alpha\beta$ system, $u_{\alpha 1}$ and $u_{\beta 1}$ are the terminal voltages of the stator in $\alpha\beta$ system, $u_{\alpha 2}$ and $u_{\beta 2}$ are the terminal voltages of the rotor in $\alpha\beta$ system. ω_r is the angular velocity of the rotor, $\Psi_{\alpha 1}$ and $\Psi_{\beta 1}$ are the flux linkage of the stator in $\alpha\beta$ system, $\Psi_{\alpha 2}$ and $\Psi_{\beta 2}$ are the flux linkage of the rotor in $\alpha\beta$ system, L_s and L_r are the self-inductance of the stator and rotor winding resistance, L_m is the mutual-inductance of the stator and rotor winding, T_e is the electromagnetic torque, T_L is the load torque, n_p is the number of pole pairs, p is the differential operator.

Eqs. (1)-(6) constituted the electromechanical coupling mathematical model of the dual-excitation fatigue loading system of wind turbine blades. This mathematical model was a non-ideal space coupling model and described the space coupling effect between the power system and vibration system during the loading process. It could be seen that the rotary driving speeds of motors, the initial phase difference of two unbalanced shafts and the mechanical properties of asynchronous motors, etc. were the factors affecting the vibration coupling.

3. Simulation analysis of the vibration coupling process

For the limited space, the influence law of driving speeds of motors and the initial phase difference of two unbalanced shafts were analyzed in simulation software Matlab/Simulink. Considering the sequent on-site test condition, the parameters of a small wind turbine blade were adopted for simulation. Moreover, symmetric installation was applied for the two set of loading equipment and the symmetric center was the point located at 70 % of the blade length along the span wise direction, namely l_{12} was equal to l_{22} in Eq. (1).

The parameters of simulation were set: $m = 29 \text{ kg}$, $m_1 = m_2 = 2 \text{ kg}$, $r = 0.15 \text{ m}$, $l_{01} = 0.05 \text{ m}$, $l_{02} = 0.25 \text{ m}$, $l_{11} = l_{21} = 0.13 \text{ m}$, $l_{12} = l_{22} = 0.32 \text{ m}$, $\beta_{01} = 45^\circ$, $\beta_{02} = 2.5^\circ$, $\beta_{11} = 42^\circ$, $\beta_{12} = 160^\circ$, $\beta_{21} = 138^\circ$, $\beta_{22} = 20^\circ$.

The initial phase difference of two unbalanced shafts was set to $\pi/2$. The rotary driving speeds of two asynchronous motors were the same and set to 150 r/min, 180 r/min, 210 r/min, 230 r/min and 260 r/min, respectively. The simulation result is shown in Fig. 3.

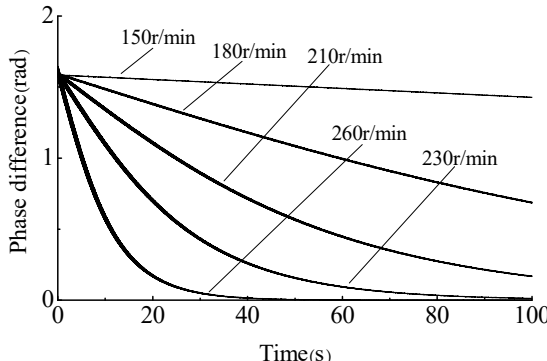


Fig. 3. Phase difference change curve at different rotary driving speed of the motors

In Fig. 3, under different rotary driving speeds, phase differences of two unbalanced shafts all gradually converged to zero. When the driving speeds of motors were 260 r/min, the phase difference converged to zero with the shortest time, about 40 s. As speeds decrease, more time would be needed for phase difference converging to zero. When the rotary driving speeds were 150 r/min, the phase difference converged to zero with long time, over 100 s. Furthermore, when the rotary driving speeds were 260 r/min, with the phase difference gradually converging to zero, the amplitude in y direction become stabilizing after a period of fluctuation, and the simulation result is shown in Fig. 4.

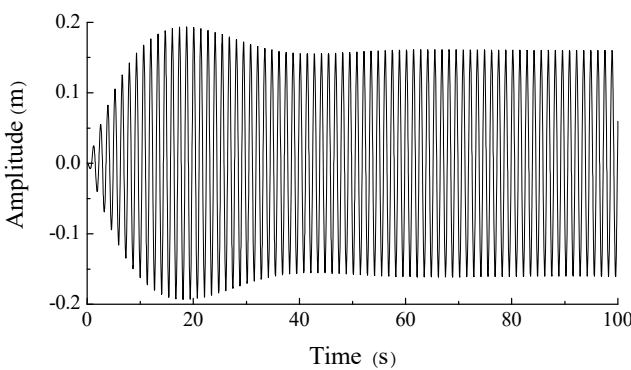


Fig. 4. The amplitude in y direction, the rotary driving speed = 260 r/min

When the rotary driving speeds of motors were set to 230 r/min and the initial phase difference of two unbalanced shafts was set to $-5\pi/6$, $-\pi/2$, $-\pi/6$, $\pi/6$, $\pi/2$, $5\pi/6$ and π , respectively. The simulation result is shown in Fig. 5.

In Fig. 5, the phase differences of the two unbalanced shafts gradually converged to zero after a period of time even the initial values were a bit large. However, when the initial value was π , the phase difference would converge to zero with longer time compared to others, and the vibration system is difficult to achieve the synchronization status. To obtain more stable amplitude, it should be avoided that the initial phase difference of the two unbalanced shafts was π .

When the rotary driving speeds of the two asynchronous motors were different from each other and set to 230 r/min and 217 r/min, respectively, the simulation result of the phase difference is shown in Fig. 6, and the amplitude result in y direction is shown in Fig. 7.

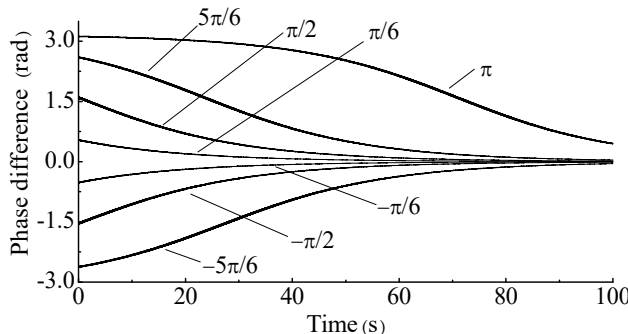


Fig. 5. Phase difference change curves under different initial values, the rotary driving speed = 230 r/min

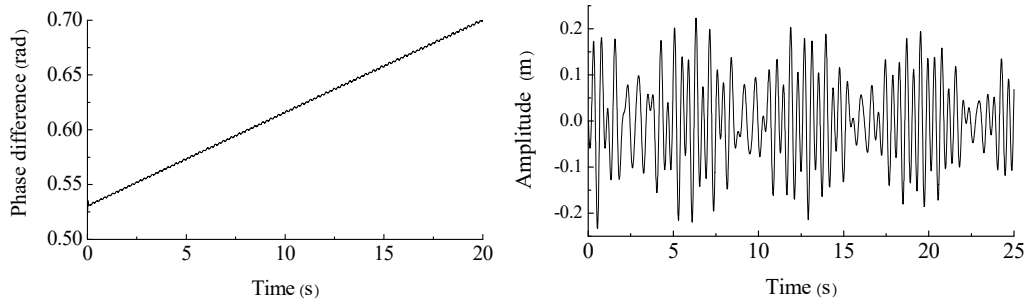


Fig. 6. The phase difference simulation result of two unbalanced shafts driven by different speeds **Fig. 7.** The amplitude simulation curve in y direction under the different speed of two motors

In Fig. 6 and Fig. 7, if the initial rotary driving speeds of two unbalance shafts were high and their speed difference was large, the two set of fatigue loading equipment could not achieve synchronization status and the amplitude in y direction could not stabilize. To obtain stable amplitude, the rotary driving speeds of two asynchronous motors should be as similar as possible, so the synchronized control of two loading sources was indispensable.

4. Test verification

To verify the correctness of the theoretical analysis and the simulation results, a small-scale dual-excitation fatigue loading system of a wind turbine blade was established. The on-site test is shown in Fig. 8 and part of test parameters is shown in Table 1.

Table 1. Test parameters

| Parameter | Value (or type) |
|---|-----------------|
| Length of the blade | 2.3 m |
| Weight of the blade (kg) | 25 |
| Weight of the unbalanced shaft (kg) | 2 |
| Equivalent arm length of the unbalanced shaft (m) | 0.15 |
| Power of the motor (kw) | 0.75 |
| Temperature (°C) | 15 |
| Humidity (RH) | 40 % |

The rotary driving speeds and phases of two unbalanced shafts were measured real-time by gear speed sensors (type: CORON-CTS). Gears with 120 teeth were installed on the motor shaft

so that the gears and the motor shaft can rotate synchronously. During the measuring, each gear speed sensor produced a pulse when a tooth of gear was detected, so the driving speeds and phases of the unbalanced shafts could be obtained. A proximity switch was installed below every unbalanced shaft to realize the reset of phase. The amplitude in y direction was measured by a laser range meter (type: ADSL-30) and the amplitude data was transferred real-time to the controller.

In this paper, Siemens S7-200 PLC was applied as the controller which calculated and analyzed the received gear pulses and amplitude data, then transmitted them to the host computer via RS485 bus. The interface of host computer was designed by LabVIEW.

During the test process, the rotary driving speeds of the two asynchronous motors were both set to 230 r/min, and the initial phase difference of the two unbalanced shafts was set to $\pi/6$. For other parameters, see the set of parameters in simulation section. The test results are shown in Fig. 9 and Fig. 10.

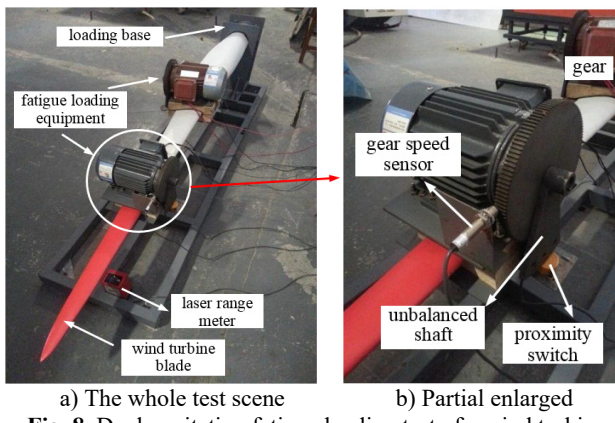


Fig. 8. Dual-excitation fatigue loading test of a wind turbine

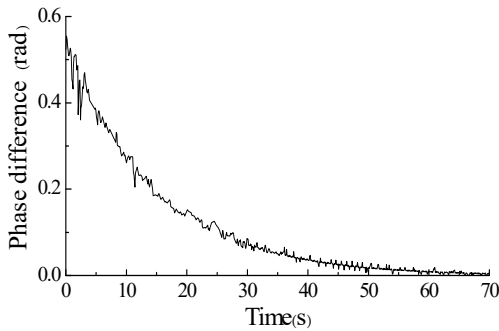


Fig. 9. Test curve of phase difference

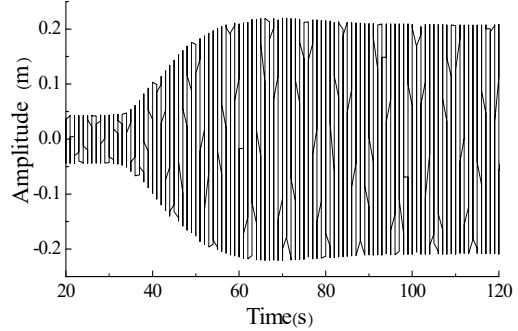


Fig. 10. The amplitude test curve in y direction

In Fig. 9 and Fig. 10, the phase difference of two unbalanced shafts gradually converged from $\pi/6$ to zero. And the amplitude in y direction gradually tended to be stable and finally kept between ± 0.25 m.

When the rotary driving speeds of two asynchronous motors were different and set to 230 r/min and 217 r/min, respectively, the test result are shown in Fig. 11 and Fig. 12.

The test result showed that the phase difference of two unbalanced shafts gradually increased if their initial driving speed difference was large. And the amplitude of the blade in y direction was disordered. The two set of fatigue loading equipment were difficult to achieve the synchronization status automatically. The test results above were consistent with the simulation results basically.

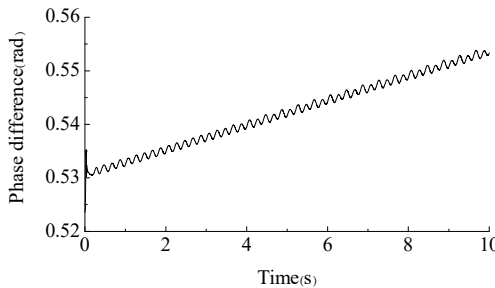


Fig. 11. The phase difference test result of two unbalanced shafts driven by different speeds

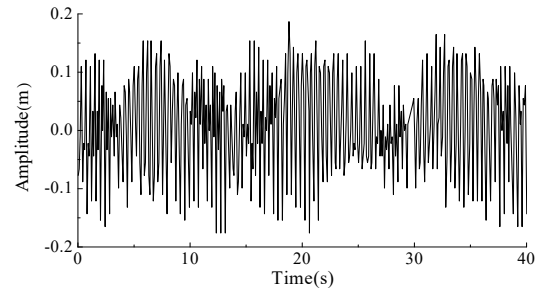


Fig. 12. The amplitude test curve in y direction under the different speed of two motors

5. Conclusion

The vibration characteristics of dual-excitation fatigue loading system of wind turbine blades was investigated, conclusions can be drawn as follows:

1) By establishing the electromechanical coupling mathematical model of the dual-excitation fatigue loading system, it was found that the main factors influencing the coupling characteristics included the initial phase difference, rotary driving speed and eccentric moment of two unbalanced shafts, the location of two set of fatigue loading equipment and the mechanical properties of asynchronous motor etc.

2) By establishing the simulation model in simulation software Matlab/Simulink, the phase differences of the two unbalanced shafts and the amplitude of the blade in y direction was obtained visually. When the rotary driving speeds of two asynchronous motors were the same, the phase difference of two unbalanced shafts gradually converged to zero, even the initial phase difference of them was not zero. What more, the higher the driving speed of motor was, the faster the phase difference converged to zero. Finally, the vibration system could step into synchronous status and at the vibrating direction, the stable amplitude could be obtained. However, it should be avoid that the initial phase difference of the two unbalanced shafts was π because a long period of time would be needed to reach the vibration synchronous status. When the initial rotary driving speeds of two asynchronous motors were high and their speed difference was large, the two set of fatigue loading equipment could not achieve synchronization status and the amplitude in y direction was disordered.

3) The results of the on-site test were consistent with the results of the simulation, which verified the correctness of the mathematical model built in this paper.

Acknowledgements

This work is sponsored by National Natural Science Foundation of China (No. 51305243) and partially supported by the Tai Shan Scholar Program.

References

- [1] <http://www.supergen-wind.org.uk/Phase1/docs/Court,%20Ridley,%20Jones,%20Bonnet%20and%20Dutton-17ICCM2009.pdf>
- [2] **Herbert G. M., Iniyian S., Revnalsan E.** A review of wind energy technologies. Renewable Sustainable Energy Reviews, Vol. 11, Issue 6, 2007, p. 1117-1145.
- [3] **Kong C., Bang J., Sugiyama Y.** Structural investigation of composite wind turbine blade considering various load cases and fatigue life. Energy, Issue 30, 2005, p. 2101-2114.
- [4] **White D., Musial W., Engberg S.** Evaluation of the new B-rex fatigue testing system for multi-megawatt wind turbine blades. 43rd AIAA Aerospace Sciences Meeting and Exhibit, USA, Vol. 6, 2005, p. 10-13.

- [5] **White D.** New Method for Dual-axis Fatigue Testing of Large Wind Turbine Blades Using Resonance Excitation and Spectral Loading. Technical Report, National Renewable Energy Laboratory (NREL), Golden, Colorado, 2004.
- [6] **Blekhman I. I., Fradkov A. L., Tomchina O. P.** Self-synchronization and controlled synchronization: general definition and example design. Mathematics and Computers in Simulation, Vol. 58, Issue 4-6, 2002, p. 367-384.
- [7] **Han Q. K., Yang X. G., Qin Z. Y., et al.** Effects of exciter parameters on self-synchronous vibration system. Journal of Northeastern University (Natural Science), Vol. 28, Issue 7, 2007, p. 1009-1012.
- [8] **Abdelghani Z. D., Dane Q.** Resonance capture in a damped three degree of freedom system: experimental and analytical comparison. International Journal of Non-Linear Mechanics, Issue 39, 2009, p. 1128-1142.
- [9] **Wang D. G., Yao H. L., Feng F., et al.** Dynamic coupling feature and experimental study of self-synchronous vibrating system. Journal of Vibration, Measurement and Diagnosis, Vol. 32, Issue S2, 2012, p. 53-58.
- [10] **Zhang N., Hou X. L., Wen B. C.** Cophase and synchronous characteristic of vibration machine under electromechanical coupling condition. Journal of Northeastern University (Natural Science), Vol. 30, Issue 10, 2009, p. 1477-1480.
- [11] **Wen B. C., Liu S. Y., Chen Z. B., et al.** Theory of Mechanical Vibration and Its Applications. Higher Education Press, Beijing, 2009.
- [12] **Pan X. S., Hao S. Y.** 50 Classic Examples of Matlab Simulation. Publishing House of Electronics Industry, Beijing, 2007.



Huang Xuemei received the B.S. degree in Mechanical Engineering from Shandong University of Technology, China, in 1997, and her M.S. and Ph.D. degrees in Mechanical Engineering from Shandong University and Shanghai Jiaotong University, China, in 2001 and 2004, respectively. She is an Associate Professor in College of Mechanical Engineering, Shandong University of Technology. Her research interests include modeling and simulation of electromechanical system, electromechanical coupling.



Zhang Lei'an received the B.S. degree in Mechanical Engineering from Weifang University, China, in 2006, and his M.S. and Ph.D. degrees in Mechanical Engineering from Shandong University of Technology and Tongji University, China, in 2009 and 2012, respectively. He is a Lecturer of College of Mechanical Engineering, Shandong University of Technology. His research is about the performance testing of wind turbine blade.



Yuan Guangming graduated in Mechanical Engineering from Nanjing University of Science and Technology, China, in 1993 and completed his Ph.D. in Mechanical Engineering from Beijing Institute of Technology, China, in 2005. Presently he is an Associate Professor in College of Mechanical Engineering, Shandong University of Technology. Presently he is interested in electro-hydraulic control system.



Wang Na received the B.S. degree in Dezhou University, Shandong, China, in 2012. Now she is a graduate student in College of Mechanical Engineering, Shandong University of Technology, China. Her current research interests include modeling and simulation of electromechanical system, the coupling and decoupling of vibration system.